Cancer Letters 316 (2012) 187–195

Contents lists available at SciVerse ScienceDirect

Cancer Letters

journal homepage: www.elsevier.com/locate/canlet

HS-116, a novel phosphatidylinositol 3-kinase inhibitor induces apoptosis and suppresses angiogenesis of hepatocellular carcinoma through inhibition of the PI3K/AKT/mTOR pathway

Kyung Hee Jung [a,1], Myung-Joo Choi [a,1], Seunghee Hong [b], Hyunseung Lee [a], Sang-Won Hong [a], Hong-Mei Zheng [a], Hee-Seung Lee [a], Sungwoo Hong [b,*], Soon-Sun Hong [a,*]

[a] Department of Biomedical Sciences, College of Medicine, Inha University, 3-ga, Sinheung-dong, Jung-gu, Incheon 400-712, Republic of Korea
[b] Department of Chemistry, Korea Advanced Institute of Science and Technology (KAIST), Daejeon 305-701, Republic of Korea

ARTICLE INFO

Article history:
Received 4 October 2011
Received in revised form 26 October 2011
Accepted 26 October 2011

Keywords:
PI3K
Apoptosis
Angiogenesis
HCC

ABSTRACT

The phosphatidylinositol 3-kinase (PI3K) pathway plays a central role in cell proliferation and survival of human cancers. As PI3K is active in many cancer patients, resulting in cancer development and progression, we developed an azaindole derivative, HS-116 as a novel PI3K inhibitor. This study aimed to clarify the anticancer effect of HS-116 in human hepatocellular carcinoma (HCC). To identify the effect of HS-116 on HCC cells, a PI3K assay, 3-(4,5-dimethylthiazol-2-yl)-2,5-diphenyltetrazolium bromide (MTT) assay, flow cytometry, and Western blotting were conducted. IC_{50} of HS-116 for PI3Kα was 31 nM, and it effectively suppressed the phosphorylation of PI3K downstream factors such as AKT, mTOR, p70S6K, and 4EBP1. Also, HS-116 induced apoptosis by increasing the proportion of sub-G1 apoptotic cells from 1.8% to 35% and increasing the expressions of Bax, cleaved-caspase-3, and cleaved-PARP as well as decreasing the expression of Bcl-2. In addition, chromatin condensation and apoptotic bodies were detected in HS-116-treated HCC cells. Furthermore, HS-116 decreased protein expression of hypoxia-inducible factor-1α (HIF-1α) and vascular endothelial growth factor (VEGF), and inhibited the tube formation and migration of human umbilical vein endothelial cells (HUVECs). *In vivo*, the ability of mice to vascularize subcutaneously implanted Matrigel plugs was diminished when the mice were treated with HS-116. These results show that HS-116 inhibits the PI3K/AKT/mTOR pathway via apoptosis and anti-angiogenesis in HCC cells. We suggest that HS-116 may be an effective novel therapeutic candidate against HCC.

1. Introduction

Hepatocellular carcinoma (HCC) is the sixth most common malignancy and the third most common cause of cancer-related mortality worldwide [1]. Being most prevalent in Asia and Africa, it is the second leading cause of cancer death in China [2] . One of the reasons for the high mortality rate in patients with HCC is the lack of effective treatment, especially for those with advanced disease. Although tumor ablation surgery can be achieved in patients with early HCC, recurrence rates are very high, approximately 50% within 3-year [3]. Also, even with treatment such as trans-arterial chemoembolization, intra-arterial or systemic chemotherapy, and radiotherapy, the 5 year relative survival rate for patients with HCC is only 7% [4]. Moreover, systemic therapy with classical cytotoxic drugs has been reported to be poorly tolerated and ineffective [5]. Especially, sorafenib, globally approved for the treatment of unrespectable and advanced HCC has shown low response rate and side effect such as hypertension, diarrhoea, rash, fatigue, and hand and foot skin reactions [6–8]. For this reason, an effective and well-tolerated pharmaceutical development for advanced HCC highlights the need for new therapeutic approaches.

In recent years, studies of an oncogenic signalling pathway that regulates cancer cell proliferation, angiogenesis, invasion, and metastasis have led to the identification of several possible therapeutic targets. The phosphoinositide 3-kinase (PI3K)/AKT/mTOR signaling pathways is one of the most commonly activated signaling pathways in human cancer [9]. PI3K catalyzes the phosphorylation of the 3-hydroxyl position of PIP2 (phosphatidylinositol 4,5-diphosphate) to PIP3 (phosphatidylinositol 3,4,5-triphosphate). Deregulation of PI3K leads to elevated PIP3 levels and downstream activation of AKT [10]. Indeed, overexpression of

* Corresponding authors. Tel.: +82 42 350 2811; fax: +82 42 350 2810 (S. Hong), tel.: +82 32 890 3683; fax: +82 32 890 2462 (S.-S. Hong).
E-mail addresses: hongorg@kaist.ac.kr (S. Hong), hongs@inha.ac.kr (S.-S. Hong).
[1] These authors contributed equally to this work.

0304-3835/$ - see front matter © 2011 Elsevier Ireland Ltd. All rights reserved.
doi:10.1016/j.canlet.2011.10.037

AKT has been established in many human cancers including HCC [11], which inhibits apoptosis and promotes cell proliferation [12]. mTOR is a serine/threonine protein kinase that exists as two functional protein complexes, mTORC1and mTORC2 [13,14]. This kinase also promotes cell growth and cell cycle progression by phosphorylating the translational regulators p70S6 kinase (p70S6K) and eukaryotic initiation factor (eIF) 4E binding protein 1 (4EBP1). To this end, PI3K/AKT/mTOR pathway has emerged as a key therapeutic target for cancer treatment. In fact, the levels of the phosphorylated form of mTOR have been shown to be elevated in 15% of cases of HCC patients, and the levels of p70S6K have been shown to be increased in 45% of the cases [15]. Therefore, the inhibition of PI3K signalling in HCC seems to be a promising strategy for the treatment.

For the goal of discovery of a new structural class of PI3K inhibitors, we initiated a pharmacophore-directed design. Our previous study reported that azaindole substructures enhance the cytotoxicity against cancer cells through stronger hydrogen bonding with the target enzymes [16]. Based on this result, we synthesized and screened a chemical library of azaindole derivatives [17]. Among them, HS-116 (N-(5-(3-(3-cyanophenyl)-1H-pyrrolo[2,3-b]pyridin-5-yl)pyridin-3-yl)benzenesulfonamide) was selected as the most potent PI3K inhibitor. In this study, we investigated whether HS-116 has anti-cancer activity against HCC, and the molecular mechanism involved in this process. Our results show that HS-116 induces apoptosis and inhibits proliferation and angiogenesis by inhibiting the of PI3K/AKT/mTOR pathway in human HCC cells.

2. Material and methods

2.1. Cells and materials

The human HCC cell lines Huh-7, Hep3B, and HepG2 were purchased from ATCC (Manassas, VA), and normal liver cell line HL-7702 was purchased from Shanghai Institute of Cell Biology (Shanghai, China). Huh-7 and HL-7702 cells were cultured in Roswell Park Memorial Institute Media 1640 (RPMI-1640), and Hep3B and HepG2 cells were cultured in Dulbecco's modified Eagle's medium (DMEM), supplemented with 10% fetal bovine serum (FBS) and 1% penicillin/streptomycin. FBS, cell culture media, penicillin–streptomycin, and all other agents used in cell culture studies were purchased from GIBCO (Grand Island, NY). Cultures were maintained at 37 °C in a CO_2 incubator with a controlled humidified atmosphere composed of 95% air and 5% CO_2. Human umbilical vein endothelial cells (HUVECs) were grown in a gelatin coated 75 cm^2 flask in M199 medium containing 20 ng/mL basic fibroblast growth factor (bFGF), 100 U/mL heparin and 20% FBS at 37 °C. Propidium iodide (PI), 3-(4,5-dimethylthiazol-2-yl)-2,5-diphenyltetrazolium bromide (MTT), and proteinase K were purchased from Sigma–Aldrich (St. Louis, MO). RNase A was purchased from Qiagen (Valencia, CA).

2.2. Synthesis of a new compound, HS-116

HS-116 was synthesized as described in our previous report [14]. Briefly, a solution of 2-chloroaniline in 20% hydrochloride was slowly added to a solution of sodium nitrite in water. Acrolein was slowly added to the reaction mixture, and then extracted with dichloromethane. The organic layers were washed with a sodium bicarbonate, dried over sodium sulfate, filtered, and evaporated to dryness to yield black viscous oil. A mixture of 2-chloro-3-(2-chlorophenyl) propanal and thiourea in ethanol was heated to reflux overnight. The solvent was removed and extracted with dichloromethane and water containing 4 M sodium hydroxide. The organic layer was extracted with 4 M hydrochloric acid to give the desired product in a 25% yield. 5-(2-chlorobenzyl) thiazol-2-amine was extracted with dichloromethane and water containing sodium bicarbonate. Next, the residue was purified using flash column chromatography (DCM:Hexane = 2:1 to only DCM) to give a desired product. The final product was more than 98% pure and was dissolved in dimethyl sulfoxide (DMSO) at a stock concentration of 50 mM, and was stored at −20 °C.

2.3. Measurement of cell proliferation

Cell viability was performed by the MTT assay. Briefly, Huh-7, Hep3B, and HepG2 cells were plated at a density of 3–5 × 10^3 cells/well in a 96-well plate for 24 or 48 h. The medium was removed, and cells were treated with either DMSO as a control or various concentrations of HS-116. The final concentration of DMSO in the medium was ⩽0.1% (v/v). After the cells were incubated for 24 or 48 h, 20 μL of the MTT solutions (2 mg/mL) was added to each well for another 4 h at 37 °C. The formazan crystals that formed were dissolved in DMSO (200 μL/well) by constant shaking for 5 min. The plate was then read on a microplate reader at 540 nm. Three replicate wells were used for each analysis. The median inhibitory concentration (IC_{50}, defined as the drug concentration at which cell growth was inhibited by 50%) was assessed from the dose–response curves.

2.4. PI3K activity assay

An active PI3K (100 ng) was preincubated with HS-116 or LY294002 for 5 min in kinase reaction buffer (3-(N-morpholino) propane sulfonic acid [MOPS, pH 7.0], 5 mM $MgCl_2$ and 1 mM ethylene glycol tetraacetic acid [EGTA]) and 10 μg L-α-phosphatidylinositol. Before addition of L-α-phosphatidylinositol, it was sonicated in water for 20 min to allow micelle formation. The reaction was started by the addition of 10 μM ATP and was run for 180 min. To terminate the kinase reaction, the same volume of Kinase-Glo® Max buffer (Promega; Madison, WI) was added. After 10 min, the plates were then read on a GloMax plate reader for luminescence detection.

2.5. Western blotting

Cells were washed three times with ice-cold phosphate buffered saline (PBS) before lysis. Cells were lysed with buffer containing 1% Triton X-100, 1% Nonidet P-40 (NP-40), and the following protease and phosphatase inhibitors: aprotinin (10 mg/mL), leupeptin (10 mg/mL) (ICN Biomedicals, Asse-Relegem, Belgium), phenylmethylsulfonyl fluoride (1.72 mM), NaF (100 mM), Na_3VO_4 (500 mM), and $Na_4P_2O_7$ (500 mg/mL) (Sigma–Aldrich, St. Louis, MO). Equal amounts of protein were separated by 10% sodium dodecyl sulfate–polyacrylamide gel electrophoresis (SDS–PAGE), transferred onto nitrocellulose membranes and the protein transfer was checked by staining with Ponceau S solution (Sigma–Aldrich). Immunostaining of the blots was performed using the primary antibodies, followed by the secondary antibody conjugated to horseradish peroxidase (HRP) and detection by enhanced chemiluminescence reagent (ELPS, Seoul, Korea). Primary antibodies were mouse monoclonal antibodies: anti-caspase-3, Bax, and Bcl-2 (Santa Cruz Biotechnology, SantaCruz, CA), anti-HIF-1α (BD Biosciences, SanJose, CA), and cleaved caspase-3, PARP, p-AKT, p-mTOR, and p-p70S6K (Cell Signaling Technologies, Danvers, MA). The secondary antibodies were purchased from Amersham Biosciences (Piscataway, NJ).

2.6. Cell cycle analysis

Huh-7 cells were plated in 100 mm-diameter culture dishes. The next day, cells were treated with various concentrations of HS-116 or 0.1% DMSO for 24 h. Floating and adherent cells were collected and fixed in cold 70% ethanol at 4 °C overnight. After washing, the cells were subsequently stained with 50 μg/mL propidium iodide (PI) and 100 μg/mL RNase A for 1 h in the dark and subjected to flow cytometric analysis to determine the percentage of cells at specific phases of the cell cycle. Flow cytometric analysis was performed using a FACSCalibur flow cytometer (Becton Dickinson, San Jose, CA) equipped with a 488 nm argon laser. Events were evaluated for each sample and the cell cycle distribution was analyzed using Cell Quest software (Becton Dickinson). The results were presented as the number of cells versus the amount of DNA as indicated by the intensity of the fluorescence signal. All the experiments were conducted three times.

2.7. DAPI staining and TUNEL assay

Huh-7 cells were plated onto an 18-mm cover glass in RPMI-1640 medium at approximately 70% confluence for 24 h. The cells were then treated with HS-116 at 10 μM for 24 h. They were fixed in ice-cold 2% para-formaldehyde (PFA), washed with PBS and then stained with 2 μg/mL 4,6-diamidino-2-phenylindole (DAPI) for 20 min at 37 °C. The stained cells were examined under a fluorescence of nuclear fragmentation. Terminal deoxynucleotidyl transferase-mediated nick end labeling (TUNEL) was performed following the manufacturer's protocol for TUNEL kit (Chemicon, Temecula, CA).

2.8. Tube formation assay

A 10 mg/mL (200 μL) of Matrigel (BD Biosciences) was polymerized for 30 min at 37 °C. HUVECs were suspended in M199 (2% FBS) medium at a density of 2.5 × 10^5 cells/mL, and 0.2 mL of cell suspension was added to each well coated with Matrigel, together with or without the indicated concentrations of HS-116 and VEGF (50 ng/mL) for 20 h. The morphological changes of the cells and tubes formed were observed under a phase-contrast microscope and photo-graphed at 200× and 400× magnification.

2.9. Wound migration assay

HUVECs plated on 60 mm-diameter culture dishes at 90% confluence, were wounded with a razor blade score 2 mm in width and marked at the injury line. After wounding, the peeled off cells were removed with a serum-free medium and further incubated in M199 with 2% FBS, 1 mM thymidine (Sigma–Aldrich), HS-116 (0.1–10 μM) and/or VEGF (50 ng/mL). HUVECs were allowed to migrate for 18 h and were rinsed with a serum-free medium, followed by fixing with absolute. Migration was quantitated with counting the number of cells that moved beyond the reference line.

2.10. Enzyme-linked immunosorbent assay (ELISA)

The amount of VEGF secreted into media was measured by sandwich ELISA. ELISA plates (Nunc, Roskilde, Denmark) were coated with 100 μL of 2 μg/mL anti-VEGF (R&D Systems, Minneapolis, MN) antibody in PBS for 24 h at 25 °C. The plates were washed with PBS containing 0.1% Tween-20 and incubated for 1 h at 25 °C with 200 μL/well of 1% bovine serum albumin (BSA, Sigma–Aldrich) in PBS. The conditioned medium or various concentrations of recombinant human VEGF were incubated for 2 h at 25 °C with 100 μL of 75 ng/mL biotinylated anti-VEGF antibody, the plates were washed and further incubated for 30 min with 100 μL of HRP-conjugated streptavidin (Vector Laboratories, Burlingame, CA). After washing, the reaction was stopped by adding 50 μL of 2 N H_2SO_4. The absorbance at 450 nm was measured with a 96-well plate reader.

2.11. Matrigel plug assay

Animal care and experimental procedures were conducted in accordance with the Guide for Animal Experiments by the Korean Academy of Medical Sciences. Male BALB/c 6-week-old mice were obtained from Orient-Bio Laboratory Animal Research Center Co., Ltd. (Gyeonggi-do, Kapyung, Korea). Animals were fed with standard rat chow with free access to tap water in a temperature- and humidity-controlled animal house alternating 12 h light–dark cycles. The mice were subcutaneously injected with 500 μL of Matrigel containing concentrated VEGF (50 ng/mL), and either HS-116 (10 μM) or PBS (10 μL). After 7 days, mice were killed and the Matrigel plugs were removed.

2.12. Histopathological examination

Matrigel plugs were fixed in 10% buffered formaldehyde, embedded in paraffin, and sectioned. The 8 μm-thick sections were stained with hematoxylin and eosin (H&E) for routine histology. For H&E staining, sections were stained with hematoxylin for 3 min, washed, and stained with 0.5% eosin for an additional 3 min. After a washing step with water, the slides were dehydrated in 70%, 96%, and 100% ethanol, and then in xylene.

2.13. Fluorescent immunohistochemistry

Ten micrometer thick frozen sections were incubated overnight at 4 °C with 1:100 dilutions of rabbit anti-p-AKT, p-p70SK, and p-4EBP antibodies (Cell Signaling Technologies). After washing three times with PBS, detection of primary antibodies were performed using a 1:200 dilution of rabbit cy5- and fluorescein isothiocynate (FITC)-labeled secondary antibodies raised in a mouse and rabbit, respectively (Vector Laboratories). After washing with PBS three times, each slide was occluded with 50% glycerin buffer and was observed using a confocal laser scanning microscope (Olympus, Tokyo, Japan).

2.14. Statistical analysis

Data are expressed as mean ± S.D. Statistical analysis was performed using ANOVA and an unpaired Student's *t*-test. A *P*-value of <0.05 was considered statistically significant. Statistical calculations were performed using SPSS for Windows Version 10.0 (SPSS, Chicago, IL).

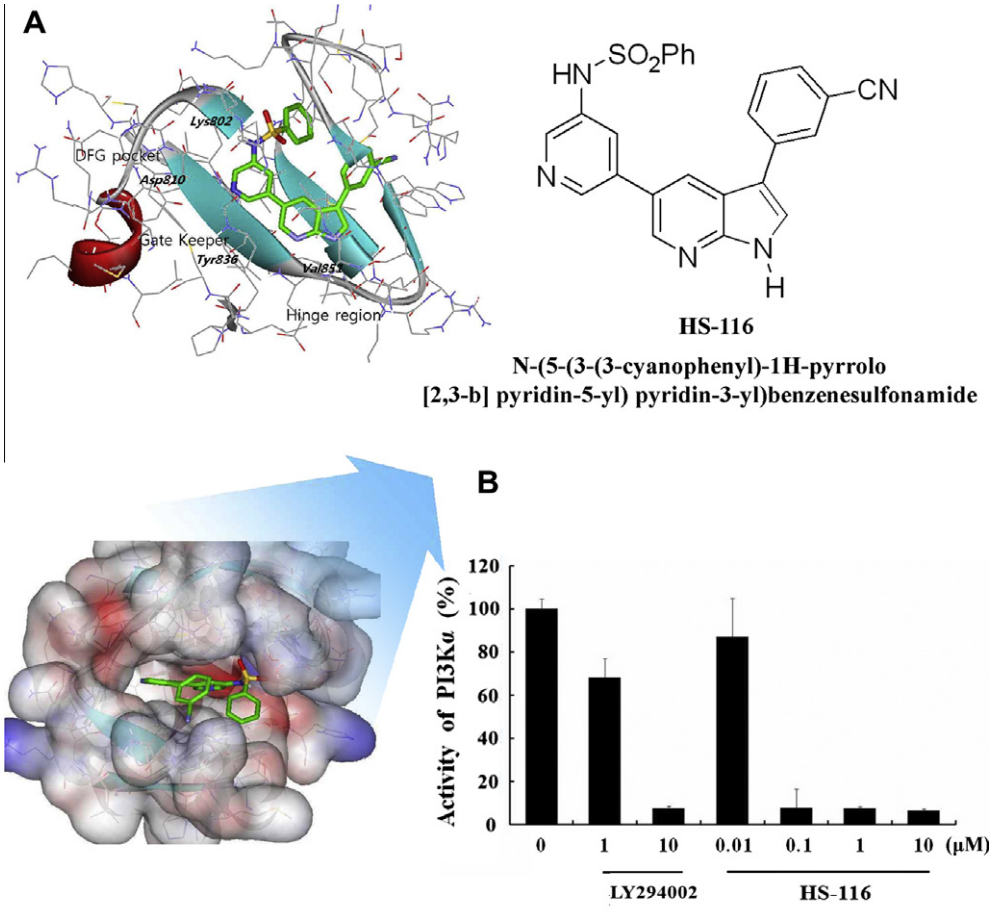

Fig. 1. Chemical structure and its docking mode of HS-116 and inhibition effects of HS-116 on phosphatidylinositol 3-kinase (PI3K) activity *in vitro*. (A) N-(5-(3-(3-cyanophenyl)-1H-pyrrolo [2,3-b]pyridin-5-yl)pyridin-3-yl) benzenesulfonamide. (B) PI3K activity was estimated using PI3-kinase ELISA kit. Data represents as mean ± S.D. from the triplicate wells.

3. Results

3.1. HS-116 inhibits PI3K activity in vitro

We synthesized a novel PI3K inhibitor HS-116, N-(5-(3-(3-cyanophenyl)-1H-pyrrolo[2,3-b]pyridine-5-pyridine-3yl) benzenesulfonamide, which inhibited comparatively ATP binding site against PI3K. We observed that HS-116 had high binding affinity in the ATP-binding site of PI3K. As shown in Fig. 1A, HS-116 appeared to be in close contact with residues Val851, Tyr836, Asp810, and Lys802, which belong to the hinge region, the gatekeeper site, DFG pocket and catalytic lysine region, respectively. Among them, these hydrogen bonds seem to play a critical role of anchor for binding of HS-116. Owing to binding of hydrogen bond at PI3K, HS-116 may be further stabilized in the ATP-binding site. We first examined the ability of HS-116 to inhibit PI3K activity *in vitro* using a PI3K assay. For these experiments, we preincubated HS-116 or LY294002, the latter a well-characterized PI3K inhibitor, for 5 min in kinase reaction buffer. The reaction was started by the addition of 10 μM ATP and L-α-phosphatidylinositol and run for 180 min. As shown in Fig. 1B, HS-116 inhibited PI3K activity dramatically. Interestingly, at concentration of 0.1 μM, HS-116 reduced the PI3K activity similar to the effect of 10 μM LY2194002. This result showed that HS-116 could act as a strong PI3K inhibitor.

3.2. HS-116 inhibits PI3K/AKT/mTOR signaling pathway in Huh-7 HCC cells

As activation of PI3K/AKT/mTOR plays a crucial role in carcinogenesis by maintaining cancer cell proliferation and preventing apoptosis [9], recent studies have focused on developing novel anti-cancer agents targeting this pathway [18,19]. Therefore, we next investigated the effects of HS-116 on the PI3K/AKT/mTOR pathway in Huh-7 HCC cells. When HCC cells were treated with various concentrations of HS-116, the phosphorylation level of AKT and its downstream factor mTOR, were effectively suppressed in a dose-dependent manner (Fig. 2A). mTOR activation results in phosphorylation of effectors such as p70S6K and 4EBP1, which subsequently leads to mTOR-dependent gene transcription that regulates cell proliferation, protein synthesis, and metabolism [20]. Therefore, we further determined the effect of HS-116 on the p70S6K and 4EBP1 using a fluorescent imaging system. The phosphorylation of p70S6K and 4EBP1 was down-regulated by HS-116 as shown by decreased fluorescence in these proteins when compared with control (Fig. 2B).

3.3. HS-116 inhibits cell growth in Huh-7 HCC cells

To determine if HS-116 could function as a new therapeutic compound, we tested the cell growth inhibition on three HCC cell

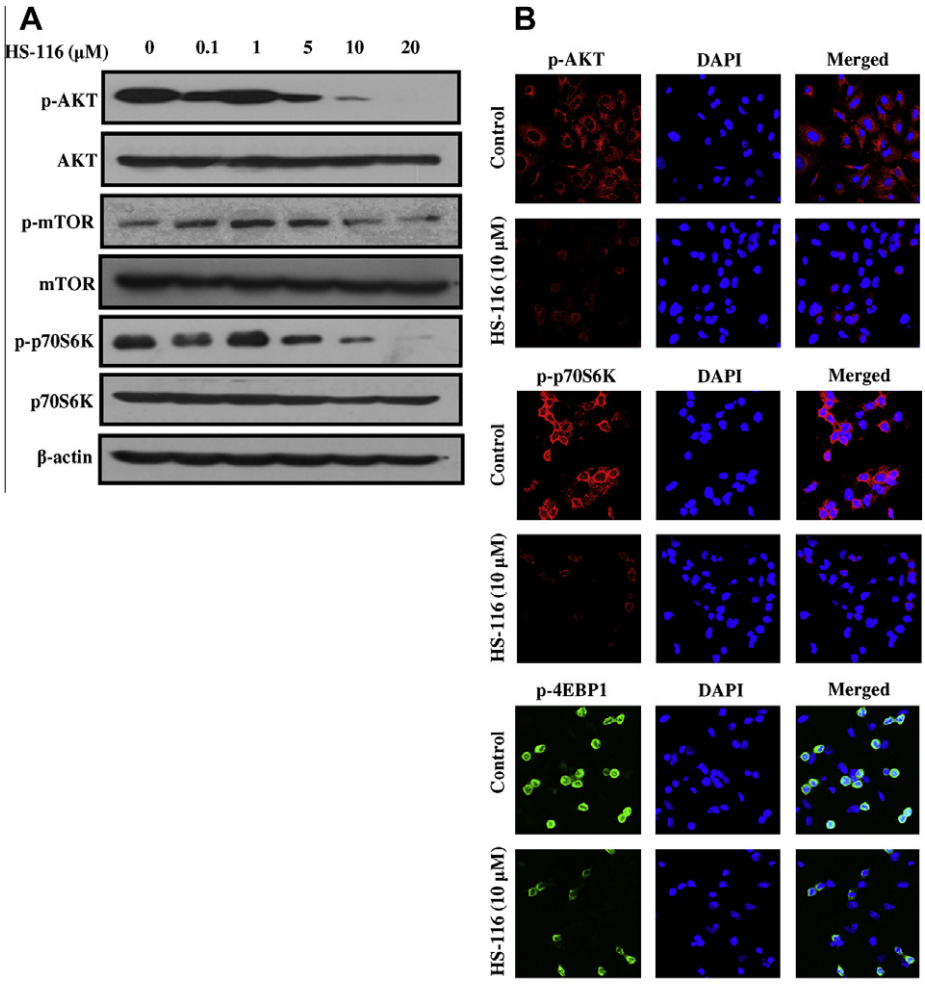

Fig. 2. Effect of HS-116 on PI3K/AKT/mTOR pathway signalling in Huh-7 HCC cells. (A) Cells were treated with HS-116 at various doses (0.1–20 μM). Western blotting experiments for p-AKT, p-mTOR, and p-p70S6K were performed with the lysates of cells. (B) Immunofluorescent imaging of PI3K/AKT/mTOR target proteins after treatment of HS-116 is shown. For labelling, anti-rabbit antibodies against p-AKT, p-70S6K, and p-4EBP1 were used. DAPI was used to counter stain the nucleus. 400× magnification.

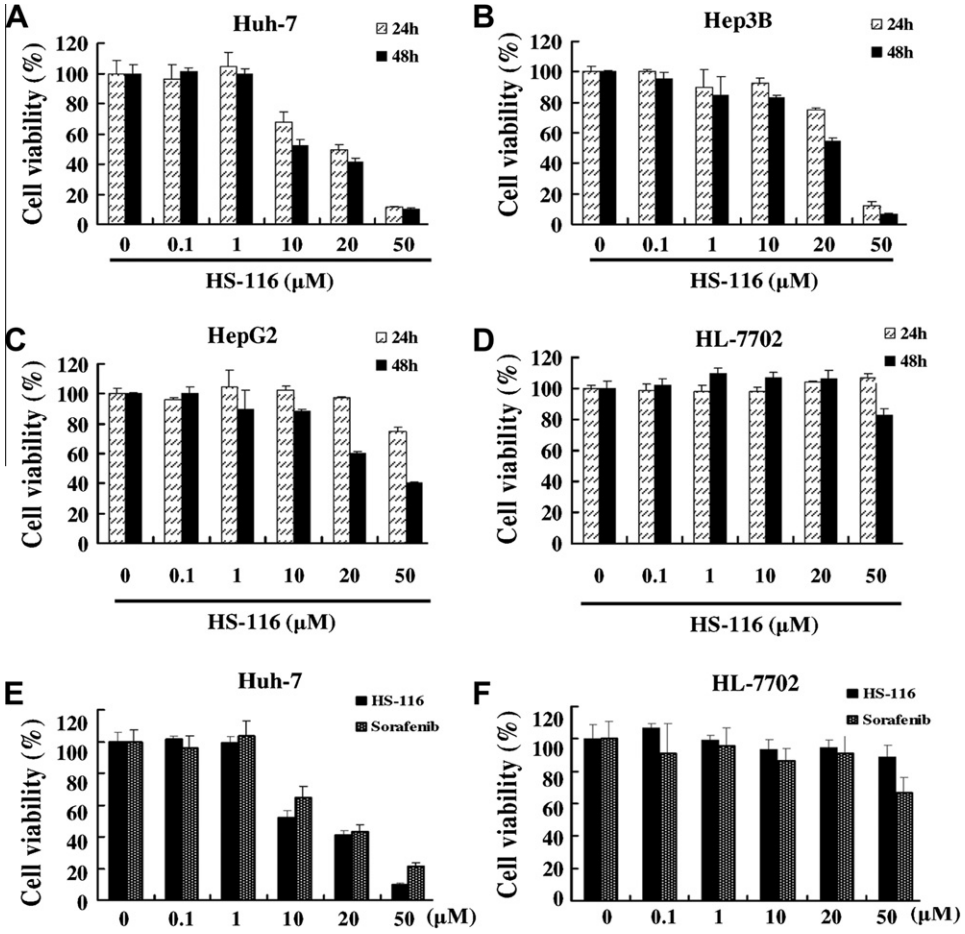

Fig. 3. Effect of HS-116 on the cell proliferation in human HCC cells and normal liver cells. (A–D) Cytotoxic effects of HS-116 on HCC cells (HepG2, Hep3B, and Huh-7) and (HL-7702). (E and F) Comparative cell viability of HS-116 and sorafenib were measured by MTT assay in Huh-7 cells and normal liver cells (HL-7702) for 48 h. HCC and normal liver cells were seeded in 96-well culture plates. After incubation for one day, the cells were treated with various concentrations of HS-116 or 0.1% dimethyl sulfoxide as a control. After incubation for 24 or 48 h, they were subjected to MTT assay. Results are expressed as percent cell proliferation relative to the proliferation of control. Data represents as mean ± S.D. from the triplicate wells.

lines (HepG2, Hep3B, and Huh-7 cells) using MTT assay. HCC cells were exposed to various concentrations (0.1–50 μM) of HS-116 for 24 h or 48 h. HS-116 treatment clearly reduced cell viability in all HCC cell lines in a time- and dose-dependent manner (Fig. 3A–C). Especially, 50 μM of HS-116 induced strong reduction in the growth rate of the three HCC cell lines which ranged between 10% and 40% at 48 h. To predict side effects of HS-116, it was exposed to HL-7702 normal liver cell line (Fig. 3D). Change of cell viability by exposure to HS-116 was less in HL-7702 than in HCC cells. Next, we compared the effects of HS-116 with those of sorafenib, a commercial drug, in Huh-7 cells. As shown in Fig. 3E, HS-116 inhibited cell growth over 20% compared with sorafenib at more than 10 μM concentration of each drug. In addition, HL-7702 cell toxicity of HS-116 (50 μM) was low (about 22%) compared with sorafenib (Fig. 3F). In summary, the effect of HS-116 was higher than sorafenib in Huh-7 HCC cells and cytotoxicity of HS-116 was lower than sorafenib in the normal liver cell line.

3.4. HS-116 induces apoptotic cell death in Huh-7 HCC cells

Cell apoptosis and growth correlated with cell cycle progression. Indeed, HS-116 induced a dose-dependent inhibition of cell growth at doses from 0.1–50 μM in Huh-7 HCC cells (Fig. 3). Thus, we performed flow cytometric analysis to determine changes of the cell cycle profile induced by HS-116. Flow cytometric data revealed that treatment with 10 and 20 μM of HS-116 increased the number of cells in subG1 phase (34–35%), indicating apoptosis and decreased G0/G1 phase in Huh-7 cells (Fig. 4A). Also, induction of apoptosis by HS-116 was evaluated by DAPI and TUNEL staining, to characterize nuclear morphology. As shown in Fig. 4B, cells treated with 10 μM HS-116 presented the characteristic morphological features of apoptotic cells, such as bright nuclear condensation and perinuclear apoptotic bodies by DAPI staining. Apoptosis by HS-116 was confirmed by detection of DNA fragmentation using TUNEL staining. We next examined the activation of caspase-3, cleaved PARP, Bax, and Bcl-2 by Western blotting after HS-116 treatment. As expected, HS-116 increased the expression of the cleaved caspase-3, cleavage of PARP, and Bax, as well decreasing the cleavage of Bcl-2 in Huh-7 HCC cells in a dose-dependent manner, starting at a concentration of 5 μM (Fig. 4C). These results showed that HS-116 could induce cell apoptosis in Huh-7 HCC cells.

3.5. HS-116 inhibits the expression of HIF-1α and VEGF in Huh-7 HCC cells

Considering the importance of HIF-1α in hypoxia and its potential correlation with HS-116, we attempted to examine the effect of HS-116 on expression pattern of HIF-1α in Huh-7 cells. Cells were treated with various concentrations of HS-116 under hypoxia-mimicking condition induced by 100 μM $CoCl_2$ for 6 h. As shown

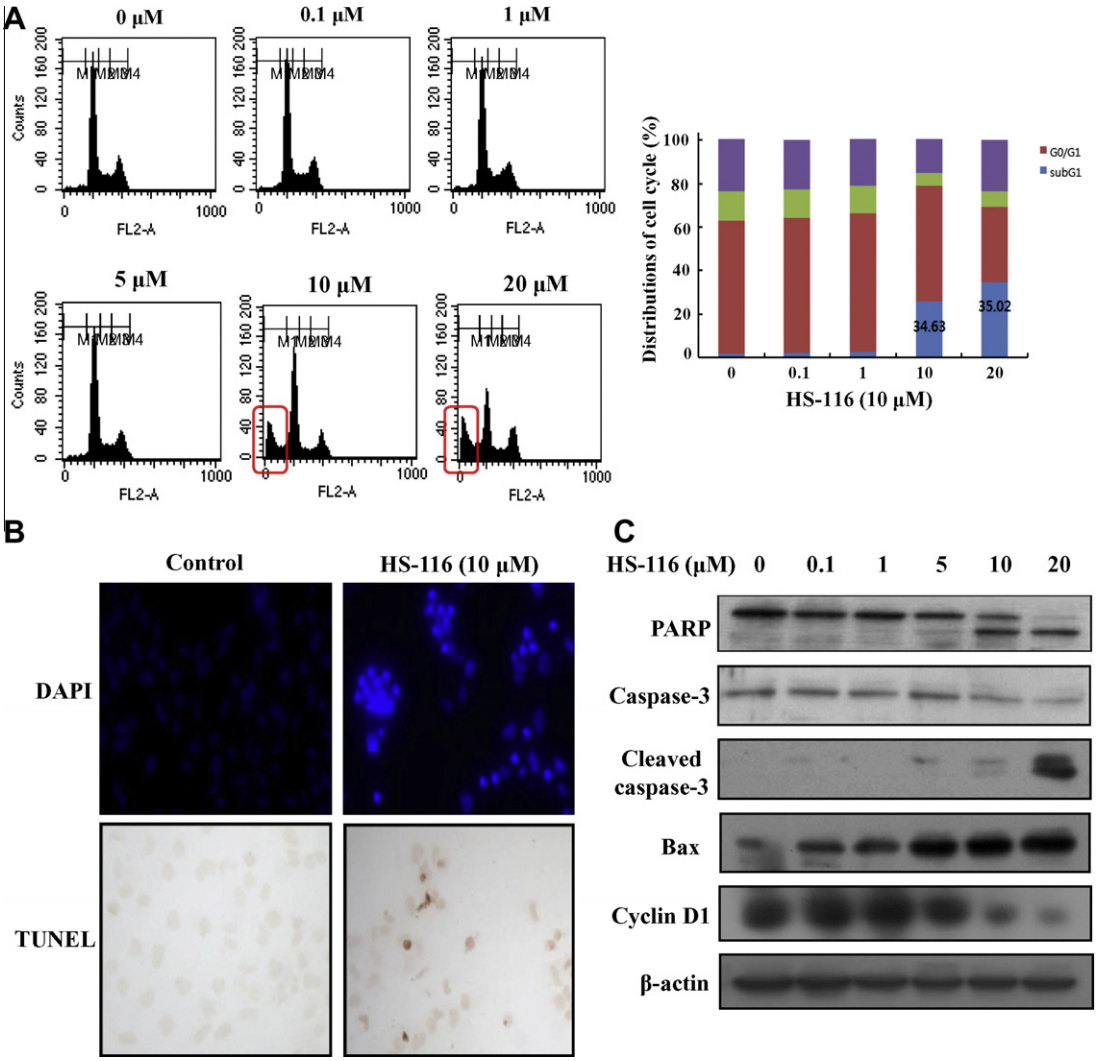

Fig. 4. Effect of HS-116 on apoptosis and cell cycle in Huh-7 HCC cells. (A) Huh-7 cells were treated with HS-116 (0, 0.1, 1, 5, 10, and 20 μM) for 48 h, stained with propidium iodide (PI) and analyzed on a FACSCalibur flow cytometer. M1, sub-G1; M2, G0/G1; M3, S; M4, G2/M. Quantitation of the PI staining data was presented as the percentages of cell cycle distribution. (B) The induction of apoptosis by HS-116 was confirmed by DAPI and TUNEL staining. Nuclear fragmentation and/or chromatin condensation was observed by DAPI staining in Huh-7 cells. Condensed and marginated chromatin was labeled to be stained dark brown in Huh-7 cells. (C) The expression of the cleaved PARP, caspase-3, and the cleaved caspase-3, Bax, and Bcl-2 were assayed by Western blotting in cells treated with HS-116 at the indicated doses for 48 h.

in Fig. 5A, HIF-1α expression was increased under the hypoxic condition. However, HS-116 in excess of 0.1 μM inhibited the hypoxia-induced HIF-1α expression. To further confirm the effect of HS-116 on hypoxia-induced VEGF, an immediate downstream target gene of HIF-1α, the protein and production of VEGF were determined by Western blotting and ELISA in Huh-7 cells. A notable increase of VEGF was observed after exposure to hypoxia, and the treatment of HS-116 suppressed hypoxia-induced VEGF expression and production in a dose-dependent manner under hypoxia (Fig. 5A and B).

3.6. HS-116 suppressed VEGF-induced tube formation and migration of HUVECs

To examine the effect of HS-116 on the angiogenesis of HCC, a capillary tube formation assay using HUVECs was done to mimic *in vivo* HCC associated angiogenesis. HS-116 inhibited VEGF-induced formation of vessel-like structures, consisting of the elongation and alignment of the cells at the indicated concentrations (Fig. 5C). Cell migration is critical for endothelial cells to form blood vessels in angiogenesis and is necessary for tumor growth and metastasis. Thus, we conducted a wound migration assay to identify the effect of HS-116 on cell migration. When the endothelial cells were wounded and incubated in a medium with VEGF in the presence of 10 μM HS-116 for 20 h, HS-116 markedly inhibited remarkably VEGF-induced cell migration (Fig. 5D). Considering that endothelial migration and tube formation are all highly relevant properties in the process of angiogenesis, our results show that HS-116 has the ability to block VEGF-induced *in vitro* angiogenesis.

3.7. HS-116 suppresses angiogenesis in the Matrigel plug model

To further confirm whether HS-116 had an anti-angiogenic activity, we performed Matrigel plug assay, which is an established *in vivo* angiogenesis model. Matrigel containing either VEGF or HS-116 was subcutaneously injected into male BALB/c mice and removed from the mice at 7 days after the implantation. As shown in Fig. 6A and B, blood vessels were rarely observed in Matrigel plugs without VEGF. VEGF strongly induced neovessels containing intact red blood cells inside the Matrigel, which were obviously inhibited by 10 μM HS-116 treatment. For histological analysis, each section of the Matrigel plug was stained with H&E and an endothelial marker CD34. The stained sections showed that the

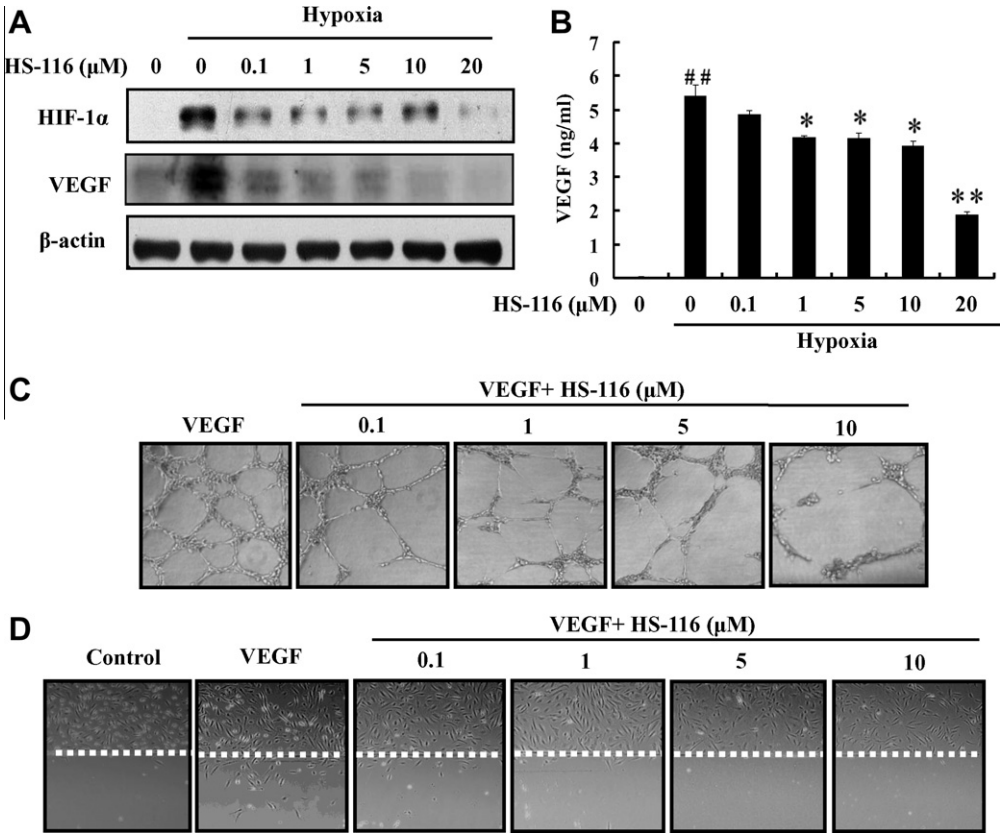

Fig. 5. Effect of HS-116 on angiogenesis of Huh-7 HCC cells. (A) Expression of HIF-1α and VEGF by HS-116 in hypoxia-induced Huh-7 cells. (B) Production of VEGF by HS-116 in hypoxia-induced Huh-7 cells for 24 h. Data represents as mean ± S.D. from the triplicate wells. $^{\#\#}P < .01$, compared to control; $^{*}P < .05$ and $^{**}P < .01$, compared to hypoxia control (C) Effects of HS-116 on VEGF-induced tube formation *in vitro*. HUVECs were plated on Matrigel (200 μL/well) and treated with various concentrations of HS-116. Capillary tube formation was assessed after 18 h. The morphological changes of the cells and tube formation were observed under a phase-contrast microscope and photographed at 200× magnification. (D) Effects of HS-116 on VEGF-induced migration *in vitro*. HUVECs were plated at 90% confluence, scratched with a razor blade.

plug with HS-116 treatment had fewer vessels within the gels than the VEGF-induced Matrigel plug. Expression of CD34 was also decreased by HS-116 treatment in VEGF-induced Matrigel plug. These results confirmed that HS-116 possessed a potent anti-angiogenic activity *in vivo*.

3.8. HS-116 inhibited the activation of VEGF-induced PI3K/AKT/mTOR signaling pathway in HUVECs

The activation of the PI3K/AKT/mTOR pathway is required for the proliferative and migratory effect of VEGF on endothelial cells [21]. Thus, we investigated the possibility that the inhibitory effect of HS-116 might be mediated through its ability to interfere with VEGF-induced activation of the PI3K/AKT/mTOR signaling pathway. To determine whether HS-116 could modulate the active signaling pathways that are involved in cell functions, HUVECs were incubated with increasing doses of HS-116 *in vitro*. When examined for the key pathway components that regulated the endothelial cell function in angiogenesis, we found that HS-116 effectively suppressed VEGF-induced activation of AKT (Fig. 6C). As a result of AKT inhibition, the activation of mTOR and p70S6K were blocked by HS-116, suggesting that HS-116 inhibits tumor angiogenesis by blocking of the PI3K/AKT/mTOR signaling pathways.

4. Discussion

The PI3K/AKT/mTOR pathway has a critical role in the pathogenesis of HCC. Indeed, the PI3K/AKT/mTOR pathway can be over-activated by enhanced stimulation of various receptor tyrosine kinase such as insulin growth like factor (IGF) and epithelial growth factor receptor (EGFR) in HCC [22]. Thus, the PI3K/AKT/mTOR pathway in cancer has been the subject of widespread and intense drug discovery for a long time [23]. Nevertheless, the optimal therapeutic strategy for targeting this pathway has not yet been identified in HCC. In this study, we developed HS-116, a novel PI3K inhibitor and explored its anticancer effects on HCC cells. For the first time, we report that HS-116 has a prominent effect on the proliferation, apoptosis, and angiogenesis through blocking the PI3K/AKT/mTOR signaling pathway in HCC.

The growth inhibitory effect is mainly mediated by inhibition of cell proliferation, which was observed in our three HCC cell lines to a similar extent at 20 μM HS-116 after 48 h. Among the three tested cell lines, Huh-7 cells were the most sensitive to HS-116. Since the PI3K/AKT/mTOR pathway regulates many different events involved in promoting cell survival and proliferation, this reduction of HCC cell proliferation by HS-116 seems to be associated with regulation of the PI3K/AKT/mTOR pathway. So, we first identified whether HS-116 inhibited PI3K (Fig. 1B) using *in vitro* kinase assay. HS-116 inhibited 50% the PI3K activity (IC_{50}) at a dose of <0.1 μM. Interestingly, the PI3K activity inhibition of HS-116 (0.1 μM) was stronger than that of LY294002 (1 μM). Considering this result, HS-116 seemed to be able to inhibit activities of AKT and mTOR, which are downstream effectors of PI3K in HCC. Indeed, when we investigated the change of the AKT and mTOR phophorylations by HS-116 in HCC cells, we discovered that HS-116 inhibited the phosphorylations of AKT and mTOR in a dose-dependent manner. In addition, it was recently reported that increased phosphorylation of 4EBP1 and p70S6K, the two best-characterized targets of mTOR, are associated with malignant disease progression

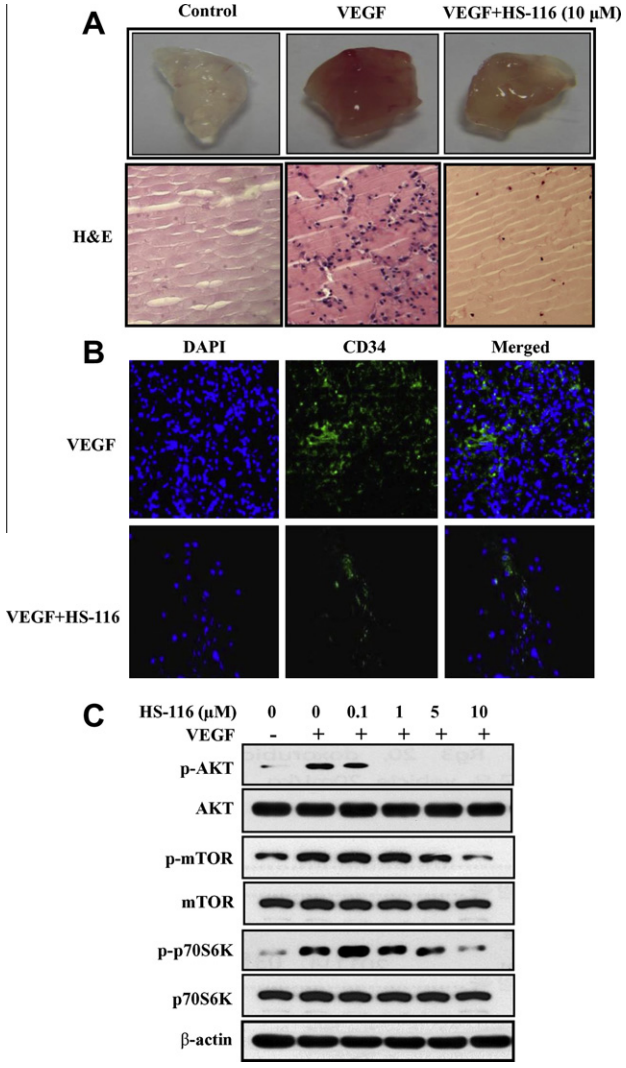

Fig. 6. Effects of HS-116 on Matrigel plug assay *in vivo* and inhibition effect of PI3K/AKT/mTOR signalling pathway by HS-116 in HUVECs. (A) Matrigel plugs were implanted into mice with VEGF (50 ng/mL) and/or HS-116 (10 μM) and then were photographed to show the extent of vascularisation after 7 days. The plugs were sectioned and stained with H&E. (B) Endothelial cells in the plug were immunostained with the CD34. A stained plug was observed by microscopy at 200× and 400× magnification (C) HS-116 inhibited the activation of PI3K/AKT/mTOR signalling pathway in HUVECs.

and adverse prognosis in various cancer patients including HCC [15,24–26]. Herein, we investigated whether HS-116 affected on p70S6K and 4EBP1, which are important in cell proliferation [27]. As expected, HS-116 apparently decreased the phosphorylations of p70S6K and 4EBP1, compared with control. The data indicates that HS-116 abrogates not only PI3K/AKT but mTOR/4EBP1 in HCC cells. We suggest that HS-116 could inhibit cell growth and proliferation by blocking the PI3K/AKT/mTOR pathway against HCC.

On the other hand, apoptosis is able to contribute to the cell growth inhibition in cancer cells. In fact, the molecular mechanisms by which anticancer drugs induce apoptosis have been reported to involve the activation of various apoptotic signalling or the inhibition of survival signalling [28,29]. So, we investigated the apoptotic effect of HS-116 and its mechanism in Huh-7 HCC cells. Bcl-2 is a critical regulator of apoptotic pathways and its overexpression is associated with many types of cancers, whereas Bax is a proapoptotic member and is translocated to mitochondria for induction of apoptosis [30]. Finally, increased Bax/Bcl-2 ratio up-regulates caspases-3, which cleaves PARP. Presently, HS-116 induced apoptosis of Huh-7 cells by increasing the expressions of the Bax, and the cleaved caspase-3 and PARP, as well as decreasing cleaved of Bcl-2. In addition, AKT is an important survival molecule in the signal pathways involved in cell growth [31] and inhibits apoptosis by inactivating various apoptotic proteins such as Bax. Considering that HS-116 inhibited phosphorylation of AKT and increased expression of apoptotic molecules such as Bax, cleaved caspase-3, and PARP, it is likely that a decreased AKT phosphorylation by HS-116 is associated with promoted cells death, indicating its apoptotic role in Huh-7 cells. Hence, we suggest that the inhibition of the PI3K/Akt pathway may be an important mechanism for anti-proliferation and the apoptosis that is induced by HS-116 in Huh-7 HCC cells.

HCC is a highly-vascularized tumor with rapid growth and repetitive vascular invasion. Angiogenesis provides a target for novel prognostic and therapeutic approaches to HCC. In the process of angiogenesis, HIF-1α plays a central role as the main regulator of the hypoxic transcription response [32]. Also, VEGF, a downstream molecule of HIF-1α, is one of many principal mediators of tumor angiogenesis [33]. So far, VEGF is the most important angiogenic factor in HCC. Tumor growth of HCC was tightly regulated by VEGF expression [34]. In addition, VEGF expression can be modulated by HIF-1α in HCC cells [35]. So, the VEGF/HIF-1α system has been considered as an important target for the anti-angiogenic therapy of HCC. In our present study, HS-116 obviously inhibited expression of HIF-1α and VEGF under hypoxia induced by $CoCl_2$ in Huh-7 cells. Angiogenesis is a complex multistep process involving endothelial cell migration, proliferation, and capillary tube formation [36]. Especially, these steps depend on the production of angiogenic factors such as VEGF in cancer [37]. Thus, we measured the anti-angiogenic effects of HS-116 on VEGF-induced migration and tube formation of endothelial cells (HUVEC) together with a Matrigel plug assay. HS-116 significantly inhibited VEGF-induced tube formation and migration of HUVECs. In addition, the anti-angiogenic effect of HS-116 was supported by decreased expression of CD34, a microvessel endothelial cell marker, in the VEGF-mediated Matrigel plug assay.

In angiogenesis, PI3K/AKT kinases are activated by various stimuli including VEGF in endothelial cells and regulate multiple critical steps by phosphorylating different downstream substrates, such as mTOR [38]. Also, the PI3K/AKT/mTOR signaling pathway is of relevance for VEGF-induced endothelial signaling [39]. Indeed, the activation of the PI3K/AKT/mTOR signaling pathway in endothelial cells promotes their survival when cultured *in vitro* [39] and in the tumor vasculature *in vivo* [40,41]. In this regard, we wondered whether HS-116 may also inhibit angiogenesis by modulating the PI3K/AKT/mTOR pathway in endothelial cells. Our result indicates that HS-116 suppresses the VEGF-induced PI3K/AKT/mTOR signalling pathway in endothelial cells, which is consistent with the report that the PI3K inhibitor NVP-BEZ235 significantly inhibits VEGF-induced AKT and p70S6K phosphorylation in endothelial cells [42]. The results indicate that HS-116 inhibits not only the expression of HIF-1α and VEGF in HCC cells but also exerts an anti-angiogenic effect on endothelial cell by inhibiting the PI3K/AKT/mTOR pathway.

In conclusion, HS-116 inhibits the PI3K/AKT/mTOR pathway and produces potent anti-HCC activity by inhibiting cell growth/proliferation and angiogenesis in parallel with increasing apoptosis. The mechanism by which HS-116 inhibits cell proliferation along with inducing apoptosis seems to be associated with inhibition of the PI3K/AKT/mTOR pathway. Thus, HS-116 may be a potential anticancer agent to inhibit the tumor progression by the targeting of the PI3K/AKT/mTOR pathway in HCC.

Role of the funding source

None declared.

Acknowledgments

This work was supported by the Korean Health Technology R&D Project (A101185) and the National R&D Program for Cancer Control (1020250), Ministry of Health & Welfare, and National Research Foundation of Korea (NRF) funded by the Ministry of Education, Science and Technology (NRF 2011-0005255, 0003609, 0016436, 0020322).

References

[1] H.B. El-Serag, K.L. Rudolph, Gastroenterology 132 (2007) 2557–2576.
[2] R.T. Poon, S.T. Fan, C.M. Lo, C.L. Liu, J. Wong, Ann. Surg. 229 (1999) 216–222.
[3] M.F. Mulcahy, Curr. Treat. Options Oncol. 6 (2005) 423–435.
[4] F.X. Bosch, J. Ribes, M. Diaz, R. Cleries, Gastroenterology 127 (2004) S5–S16.
[5] C. Verslype, E. Van Cutsem, M. Dicato, N. Arber, J.D. Berlin, D. Cunningham, A. De Gramont, E. Diaz-Rubio, M. Ducreux, T. Gruenberger, D. Haller, K. Haustermans, P. Hoff, D. Kerr, R. Labianca, M. Moore, B. Nordlinger, A. Ohtsu, P. Rougier, W. Scheithauer, H.J. Schmoll, A. Sobrero, J. Tabernero, C. van de Velde, Ann. Oncol. 20 (Suppl. 7) (2009) vii1–vii6.
[6] A.L. Cheng, Y.K. Kang, Z. Chen, Lancet Oncol. 10 (2009) 25–34.
[7] J.M. Llovet, S. Ricci, V. Mazzaferro, P. Hilgard, E. Gane, J.F. Blanc, A.C. de Oliveira, A. Santoro, J.L. Raoul, A. Forner, N. Engl. J. Med. 359 (2008) 378–390.
[8] R. Kim, M.T. Byrne, A. Tan, Oncology 25 (2011) 283–291.
[9] T.A. Yap, M.D. Garrett, M.I. Walton, F. Raynaud, J.S. de Bono, P. Workman, Curr. Opin. Pharmacol. 8 (2008) 393–412.
[10] C. Bohmer, F. Wehner, FEBS Lett. 494 (2001) 125–128.
[11] K. Oda, J. Okada, L. Timmerman, P. Rodriguez-Viciana, D. Stokoe, K. Shoji, Y. Taketani, H. Kuramoto, Z.A. Knight, K.M. Shokat, F. McCormick, Cancer Res. 68 (2008) 8127–8136.
[12] S.R. Datta, A. Brunet, M.E. Greenberg, Genes Dev. 13 (1999) 2905–2927.
[13] E.A. Dunlop, A.R. Tee, Cell. Signal. 21 (2009) 827–835.
[14] C.A. Sparksm, D.A. Guertin, Oncogene 29 (2010) 3733–3744.
[15] F. Sahin, R. Kannangai, O. Adegbola, J. Wang, G. Su, M. Torbenson, Clin. Cancer Res. 10 (2004) 8421–8425.
[16] C. Marminon, A. Pierre, B. Pfeiffer, V. Perez, S. Leonce, P. Renard, M. Prudhomme, Bioorg. Med. Chem. 11 (2003) 679–687.
[17] S. Hong, S. Lee, B. Kim, H. Lee, S.S. Hong, S. Hong, Bioorg. Med. Chem. Lett. 20 (2010) 7212–7215.
[18] D.C. Cho, M.B. Cohen, D.J. Panka, M. Collins, M. Ghebremichael, M.B. Atkins, S. Signoretti, J.W. Mier, Clin. Cancer Res. 16 (2010) 3628–3638.
[19] S. Whittaker, R. Marais, A.X. Zhu, Oncogene 29 (2010) 4989–5005.
[20] S. Huang, P.J. Houghton, Curr. Opin. Pharmacol. 3 (2003) 371–377.
[21] M.J. Cross, L. Claesson-Welsh, Trends Pharmacol. Sci. 22 (2001) 201–207.
[22] C. Alexia, G. Fallot, M. Lasfer, G. Schweizer-Groyer, A. Groyer, Biochem. Pharmacol. 68 (2004) 1003–1015.
[23] P. Wu, T. Liu, Y. Hu, Curr. Med. Chem. 16 (2009) 916–930.
[24] J.R. Graff, B.W. Konicek, R.L. Lynch, C.A. Dumstorf, M.S. Dowless, A.M. McNulty, S.H. Parsons, L.H. Brail, B.M. Colligan, J.W. Koop, B.M. Hurst, J.A. Deddens, B.L. Neubauer, L.F. Stancato, H.W. Carter, L.E. Douglass, J.H. Carter, Cancer Res. 69 (2009) 3866–3873.
[25] F. Rojo, L. Najera, J. Lirola, J. Jimenez, M. Guzman, M.D. Sabadell, J. Baselga, S. Ramon, Y. Cajal, Clin. Cancer Res. 13 (2007) 81–89.
[26] J. Castellvi, A. Garcia, F. Rojo, C. Ruiz-Marcellan, A. Gil, J. Baselga, S. Ramon, Y. Cajal, Cancer 107 (2006) 1801–1811.
[27] R.J. Dowling, I. Topisirovic, T. Alain, M. Bidinosti, B.D. Fonseca, E. Petroulakis, X. Wang, O. Larsson, A. Selvaraj, Y. Liu, S.C. Kozma, G. Thomas, N. Sonenberg, Science 328 (2010) 1172–1176.
[28] M.C. Cabot, A.E. Giuliano, T.Y. Han, Y.Y. Liu, Cancer Res. 59 (1999) 880–885.
[29] M. Selzner, A. Bielawska, M.A. Morse, H.A. Rudiger, D. Sindram, Y.A. Hannun, P.A. Clavien, Cancer Res. 61 (2001) 1233–1240.
[30] P.C. Ashe, M.D. Berry, Prog. Neuropsychopharmacol. Biol. Psychiatry 27 (2003) 199–214.
[31] M. Osaki, M. Oshimura, H. Ito, Apoptosis 9 (2004) 667–676.
[32] G.L. Semenza, Nat. Rev. Cancer 3 (2003) 721–732.
[33] J. Fang, M. Ding, L. Yang, L.Z. Liu, B.H. Jiang, Cell. Signal. 19 (2007) 2487–2497.
[34] H. Yoshiji, S. Kuriyama, J. Yoshii, M. Yamazaki, M. Kikukawa, H. Tsujinoue, T. Nakatani, H. Fukui, Hepatology 28 (1998) 1489–1496.
[35] L. Lu, Z. Yang, B. Zhu, S. Fang, X. Yang, W. Cai, C. Li, J.X. Ma, G. Gao, Cancer Lett. 257 (2007) 97–106.
[36] C.H. Blood, B.R. Zetter, Biochim. Biophys. Acta 1032 (1990) 89–118.
[37] P. Carmeliet, Nat. Med. 9 (2003) 653–660.
[38] D.H. Cho, Y.J. Choi, S.A. Jo, J. Ryou, J.Y. Kim, J. Chung, I. Jo, Am. J. Physiol. Cell Physiol. 291 (2006) C317–326.
[39] A.K. Olsson, A. Dimberg, J. Kreuger, L. Claesson-Welsh, Nat. Rev. Mol. Cell Biol. 7 (2006) 359–371.
[40] L.E. Benjamin, E. Keshet, Proc. Natl Acad. Sci. USA 94 (1997) 8761–8766.
[41] Y. Nakahara, Kango Gijutsu. 26 (1980) 2047–2050.
[42] C.R. Schnell, F. Stauffer, P.R. Allegrini, T. O'Reilly, P.M. McSheehy, C. Dartois, M. Stumm, R. Cozens, A. Littlewood-Evans, C. Garcia-Echeverria, S.M. Maira, Cancer Res. 68 (2008) 6598–6607.